

8-2023

## **Modulation of Voltage-Gating and Hysteresis of Lysenin Channels by $\text{Cu}^{2+}$ Ions**

Andrew Bogard  
*Boise State University*

Pangaea W. Finn  
*Boise State University*

Aviana R. Smith  
*Boise State University*

Ilinca M. Flacau  
*Boise State University*

Rose Whiting  
*Boise State University*

*See next page for additional authors*

---

**Authors**

Andrew Bogard, Pangaea W. Finn, Aviana R. Smith, Ilinca M. Flacau, Rose Whiting, and Daniel Fologea



Article

# Modulation of Voltage-Gating and Hysteresis of Lysenin Channels by $\text{Cu}^{2+}$ Ions

Andrew Bogard<sup>1,2</sup>, Pangaea W. Finn<sup>1</sup>, Aviana R. Smith<sup>1</sup> , Ilinca M. Flacau<sup>1</sup>, Rose Whiting<sup>1,2</sup>  
and Daniel Folegea<sup>1,2,\*</sup>

<sup>1</sup> Department of Physics, Boise State University, Boise, ID 83725, USA

<sup>2</sup> Biomolecular Sciences Graduate Program, State University, Boise, ID 83725, USA

\* Correspondence: danielfolegea@boisestate.edu

**Abstract:** The intricate voltage regulation presented by lysenin channels reconstituted in artificial lipid membranes leads to a strong hysteresis in conductance, bistability, and memory. Prior investigations on lysenin channels indicate that the hysteresis is modulated by multivalent cations which are also capable of eliciting single-step conformational changes and transitions to stable closed or sub-conducting states. However, the influence on voltage regulation of  $\text{Cu}^{2+}$  ions, capable of completely closing the lysenin channels in a two-step process, was not sufficiently addressed. In this respect, we employed electrophysiology approaches to investigate the response of lysenin channels to variable voltage stimuli in the presence of small concentrations of  $\text{Cu}^{2+}$  ions. Our experimental results showed that the hysteretic behavior, recorded in response to variable voltage ramps, is accentuated in the presence of  $\text{Cu}^{2+}$  ions. Using simultaneous AC/DC stimulation, we were able to determine that  $\text{Cu}^{2+}$  prevents the reopening of channels previously closed by depolarizing potentials and the channels remain in the closed state even in the absence of a transmembrane voltage. In addition, we showed that  $\text{Cu}^{2+}$  addition reinstates the voltage gating and hysteretic behavior of lysenin channels reconstituted in neutral lipid membranes in which lysenin channels lose their voltage-regulating properties. In the presence of  $\text{Cu}^{2+}$  ions, lysenin not only regained the voltage gating but also behaved like a long-term molecular memory controlled by electrical potentials.

**Keywords:** pore-forming toxins; lysenin; voltage gating; hysteresis; memory; bistability;  $\text{Cu}^{2+}$  ions



**Citation:** Bogard, A.; Finn, P.W.; Smith, A.R.; Flacau, I.M.; Whiting, R.; Folegea, D. Modulation of Voltage-Gating and Hysteresis of Lysenin Channels by  $\text{Cu}^{2+}$  Ions. *Int. J. Mol. Sci.* **2023**, *24*, 12996. <https://doi.org/10.3390/ijms241612996>

Academic Editors: Marco Colombini and Sergey M. Bezrukov

Received: 18 June 2023

Revised: 12 August 2023

Accepted: 18 August 2023

Published: 20 August 2023



**Copyright:** © 2023 by the authors. Licensee MDPI, Basel, Switzerland. This article is an open access article distributed under the terms and conditions of the Creative Commons Attribution (CC BY) license (<https://creativecommons.org/licenses/by/4.0/>).

## 1. Introduction

Lysenin is a protein extracted from the coelomic fluid of the earthworm *E. fetida*, which inserts large  $\beta$ -barrel pores in artificial and natural lipid membranes [1–6]. The intricate, multi-step mechanism of pore formation implies binding to sphingomyelin (SM), oligomerization into prepores, and prepore-to-pore conversion [4,6–9]. The large diameter of the conducting pathway of the pore (~3 nm, [1,3,5]) leads to uncontrolled leakage of ions and molecules; this strong lytic activity dubbed lysenin as a pore-forming toxin (PFT) [5,7–10], although its physiological role is yet to be deciphered.

Reconstituted lysenin channels share features specific to ion channels such as large transport rate, regulation, and selectivity [2,10–14]. The intrinsic regulatory mechanisms manifest by adjustments of the channel's conformation and conductance in response to stimuli of physical and chemical origin [13–15]. Lysenin channels reconstituted in artificial membrane systems comprising anionic lipids present voltage-induced gating at low positive voltages [2,16,17], but this feature vanishes when the channels are reconstituted in neutral membranes [2,11]. When exposed to multivalent cations, lysenin channels present ligand-induced gating in both charged and neutral lipid membranes [11,13,15].

A salient feature of lysenin channels is the prominent hysteresis in conductance and bistability, indicative of molecular memory [16–19]. Hysteresis manifests when the response to a particular stimulation is not fixed and depends on the history of the system [20].

All voltage-gated ion channels characterized by two states (i.e., open and closed) may present a dynamic hysteresis in conductance, resulting from the slow equilibration of the channels in response to periodic voltage stimuli [21]. However, other intrinsic mechanisms may come into play and endow ion channels with a more persistent hysteresis [20,22,23]. Any hysteretic behavior leads to bistability and acquisition of memory emerging from the history-dependent behavior [18,20,23], which paves the way for gaining novel functionalities originating in the non-Markovian distribution of the states explorably by the system under investigations.

In the case of lysenin, the observed hysteresis is not dynamic, and seemingly originates in an invariant reopening pathway of the channels previously closed by applied positive voltages [16,18]. Notably, the reactivation pathway is also temperature-independent, while the inactivation pathway is strongly modulated by temperature variations [18]. This memristor-like behavior [18,24,25] manifests at time scales that greatly exceed the hysteresis observed for ion channels [26–30]. The hysteresis in conductance of lysenin does not vanish when the period of the oscillatory voltage stimulus is much larger than the relaxation time of the channels [18], which would be the hallmark of dynamic hysteresis [21].

The hysteretic behavior of lysenin channels is intimately linked to two important regulatory mechanisms, unique among PFTs, namely, voltage-induced gating and ligand-induced gating. To date, no reasonable attempt to advance a realistic model of lysenin regulation has been made, and this is justified by the multiple challenges accompanying such an attempt. A realistic model of gating must account for all regulatory features investigated so far regarding voltage gating, ligand gating, and hysteretic behavior. However, the regulatory response to physical and chemical factors is far from uniform.  $K^+$  ions and higher pH lead to a right shift in the voltage-induced gating, suggesting modulation of voltage regulation by electrostatic interactions [14]. The same monovalent cations adjust the hysteresis in conductance by shifting the voltage needed to close the channels to higher values, yet the reactivation pathway is rather invariant [16]. Multivalent ions present a more intricate interaction with lysenin channels, dominated by the resulting ligand-induced gating [11,13,15,31]. Many trivalent metal cations (lanthanides,  $Al^{3+}$ ,  $Fe^{3+}$ ) force the individual channels to adopt a fully closed state, while divalent metal cations ( $Ca^{2+}$ ,  $Mg^{2+}$ , etc.) induce stable conformational changes characterized as sub-conducting states [11,13,15]. In most cases, the inhibitory effects are suppressed upon ligand removal by precipitation or chelation, indicative of reversibility. However,  $Cr^{3+}$  ions present a distinct inhibition pattern, suggesting cooperativity, and the changes are not reversible [15]. In the same line of intricacy, voluminous organic cations (spermidine, spermine) present an inhibition profile resembling divalent metal cations [13,15], suggesting that charge density as opposed to charge alone influences the pathway adopted for conformational changes (i.e., full closing, as opposed to sub-conducting).  $La^{3+}$  ions, at concentrations sufficiently small to render ligand-induced gating negligible, influence hysteresis similarly to monovalent cations: a right shift of the voltage gating and open probability during ascending voltage ramps, and a rather invariant reopening pathway during descending voltage ramps [16]. The interaction with anionic ATP adds another level of intricacy: the conductance is inhibited in a concentration-dependent manner, yet voltage-gating and open probability show a strong right shift for both ascending and descending voltage ramps [16,31].

These prior investigations are indicative of major hurdles in elaborating a realistic model of gating, yet they may provide clues required for a better understanding of regulatory mechanisms and hysteretic response. We attempted to explain gating and hysteretic behavior by considering electrostatic screening of a voltage-domain sensor moving into the hydrophobic core of the membrane [16], but no strong evidence for such a mechanism exists. Therefore, any additional clue on lysenin's functionality modulation by physical or chemical cues may contribute to the development of a realistic model of regulation. To gain new knowledge on the functionality of lysenin channels, we employed electrophysiology approaches to assess the effect of  $Cu^{2+}$  ions on the voltage regulation and hysteretic behavior. Unlike other multivalent metals that force the channels to close in a single step or to

adopt a stable, sub-conducting state [11],  $\text{Cu}^{2+}$  ions interact with lysenin and lead to full closing in two steps [11,13]. To verify if this distinct interaction between lysenin channels and  $\text{Cu}^{2+}$  ions influences the hysteresis in conductance, we employed electrophysiology measurements and concluded that the addition of small amounts of  $\text{Cu}^{2+}$  ions not only significantly enhances the hysteretic behavior but also enables its persistent manifestation at zero bias voltage. This result prompted us to further investigate the effect of  $\text{Cu}^{2+}$  ions on the voltage-gating of lysenin channels reconstituted in neutral membranes, for which such feature is abrogated [2,11,15]. Surprisingly,  $\text{Cu}^{2+}$  addition led to a full restoration of the voltage-induced gating of lysenin channels reconstituted in neutral membranes, which also manifested a strong hysteresis in conductance.

## 2. Results and Discussion

Our experiments were initiated by reconstituting lysenin channels in a planar Bilayer Lipid Membrane (BLM) composed of Asolectin (Aso), Sphingomyelin (SM), and Cholesterol (Chol), bathed by electrolyte solutions (50 mM KCl, 20 mM Hepes, pH 7.2). We opted for a low electrolyte concentration for several reasons: lysenin channels gate at lower voltages [14,16], a low conductivity solution enables measuring ionic currents through very large populations of reconstituted channels [19], and a lower ionic strength may enhance the electrostatic interactions by reducing screening. Channel insertion was monitored at  $-60$  mV bias potential, and the insertion of individual channels was inferred from the stepwise variation of the ionic currents (Figure 1). Each inserted channel led to a variation of the ionic current by  $\sim 20$  pA, consistent with previous experiments carried out in similar solution and electrical conditions [19]; the resulting conductance ( $\sim 0.33$  nS/channel) was used to provide a rough yet realistic estimation of the number of reconstituted channels for each of the experiments from the slope of the linear portion of the I-V plots [13,19] or the macroscopic currents measured at a voltage at which all the channels are fully conducting.

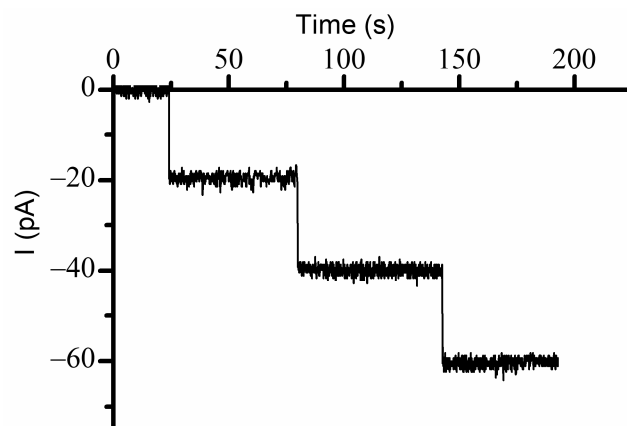


**Figure 1.** Lysenin inserts uniform channels in artificial lipid membranes. The insertion of individual lysenin channels in a planar bilayer lipid membrane was monitored from the stepwise variation of the ionic currents at  $-60$  mV transmembrane voltage. Each inserted channel adjusted the ionic current by  $\sim 20$  pA.

The next investigations focused on recording the response of a population of  $\sim 1300$  lysenin channels to a slow oscillatory voltage stimulus in the positive voltage range with and without addition of  $\text{Cu}^{2+}$  ions. For this task, we measured the ionic currents in response to linearly variable voltage ramps (ascending and descending) ranging from 0 mV to  $+60$  mV with a period of 20 min at a sampling rate of 1 Hz, a protocol customarily used to assess the hysteretic behavior of lysenin's conductance [16]. In the absence of  $\text{Cu}^{2+}$  ions (control experiment), the lysenin channels showed the typical hysteretic behavior [16,18] (Figure 2a). During the ascending voltage ramp, the currents increased linearly with voltage until  $\sim 20$  mV, after which the channels started to close, and the ionic currents became negligible at voltages greater than 45 mV. The closed channels started reopening at lower voltages

during the descending voltage ramp, and full reopening occurred at voltages under 10 mV. Given the known influence presented by monovalent and trivalent metal cations on the hysteretic conductance of lysenin channels [16], we expected  $\text{Cu}^{2+}$  ions to elicit a right shift in the voltage gating during the ascending voltage ramp, and an invariant reopening pathway during the descending voltage ramp. However, the I-V plot recorded in response to otherwise identical voltage ramps after  $\text{Cu}^{2+}$  addition was quite different (Figure 2a): the channels started closing at a much lower voltage (<10 mV) during the ascending voltage ramp, and minimal reopening occurred during the descending voltage ramp. The hysteresis in conductance persisted but the channels resisted reopening after  $\text{Cu}^{2+}$  addition.

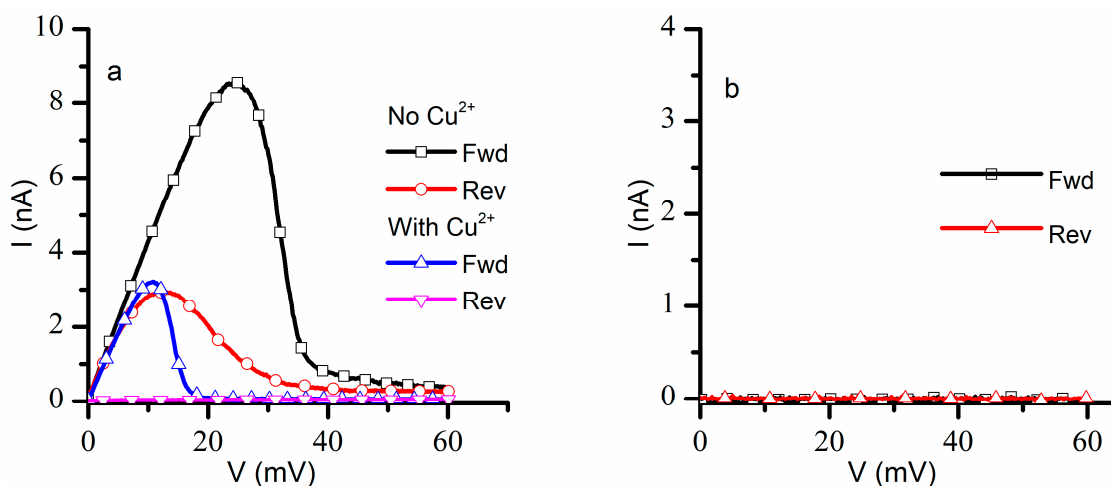


**Figure 2.**  $\text{Cu}^{2+}$  ions adjust the voltage gating and hysteresis in the positive voltage range. (a) The I-V plots recorded for forward and reverse voltage ramps before and after  $\text{Cu}^{2+}$  addition indicate major adjustments in channel closing and reopening.  $\text{Cu}^{2+}$  addition reduces the voltage required to initiate gating during ascending (Fwd) voltage ramps and elicit resistance to reopening during descending voltage ramps (Rev). (b) The negligible ionic currents recorded for a consecutive voltage ramp applied to  $\text{Cu}^{2+}$ -exposed channels indicates the persistency of the closed state of the channels. The panels show experimental data from single traces, with the symbols added to facilitate identification.

A consistent overlap of the I-V plots was observed for three consecutive runs within the same experiment in the absence of  $\text{Cu}^{2+}$  ions. However, the I-V plots recorded after  $\text{Cu}^{2+}$  addition changed significantly following the first run: the closed channels did not reopen after the first run, and only negligible ionic currents were recorded for both ascending and descending voltage ramps (Figure 2b). The attempt to record data from independent experiments proved futile, owing to difficulties to replicate the exact same number of inserted lysenin channels in independent experiments. The insertion process is not easily controlled, and the number of inserted channels may differ substantially between experiments carried out in otherwise identical experimental conditions, which would make a statistical analysis of I-V plots meaningless. One may argue that a normalized value, like the open probability, would be suitable for statistical analyses of data from independent experiments; this is not necessarily true, since it was shown that the open probability may depend on the number of inserted channels [19]. Consequently, our results represent typical, single traces recorded in individual experiments. However, each set of paired data showing the effects of  $\text{Cu}^{2+}$  on a particular feature comprised the same membrane, with measurements taken before and after  $\text{Cu}^{2+}$  addition. This limitation is not uncommon: single traces are reported for similar electrophysiology experiments in which the number of channels cannot be precisely controlled [27–29,32], including plots of normalized quantities.

For a better understanding of the effects presented by  $\text{Cu}^{2+}$  ions on gating, we repeated the experiments by extending the voltage range from  $-80$  mV to  $+80$  mV and the ramp period to 30 min (Figure 3) for a population of  $\sim 950$  channels. In the absence of  $\text{Cu}^{2+}$  ions, the I-V plot recorded in response to the ascending voltage ramp showed the typical

response of lysenin channels to external voltages [14,16,18,19]. From  $-80$  mV to  $+20$  mV, the ohmic relationship between macroscopic currents and voltages indicated that the channels remained in the open state (Figure 3a). The channels began to close at voltages exceeding  $+20$  mV; this behavior continued up to the maximum applied voltage of  $+80$  mV. The steep decrease in the macroscopic currents at voltages over  $+30$  mV indicated voltage gating and sustained channel closure; the effectiveness of voltage gating at positive potentials was inferred from the very small ionic currents recorded at voltages greater than  $+50$  mV. After nearly all the channels were closed by the large depolarizing voltage, the application of a descending voltage (from  $+80$  mV to  $-80$  mV) led to the observation of hysteresis in conductance (Figure 3a). The reopening of the lysenin channels followed a different pathway: the channels showed a preference for the closed state for a larger voltage range and fully reopened at lower positive voltages. At descending voltages under  $\sim +8$  mV, the linear I-V plot indicated an ohmic behavior identical to the I-V plot recorded for ascending voltages, confirming a complete reopening of the channels.

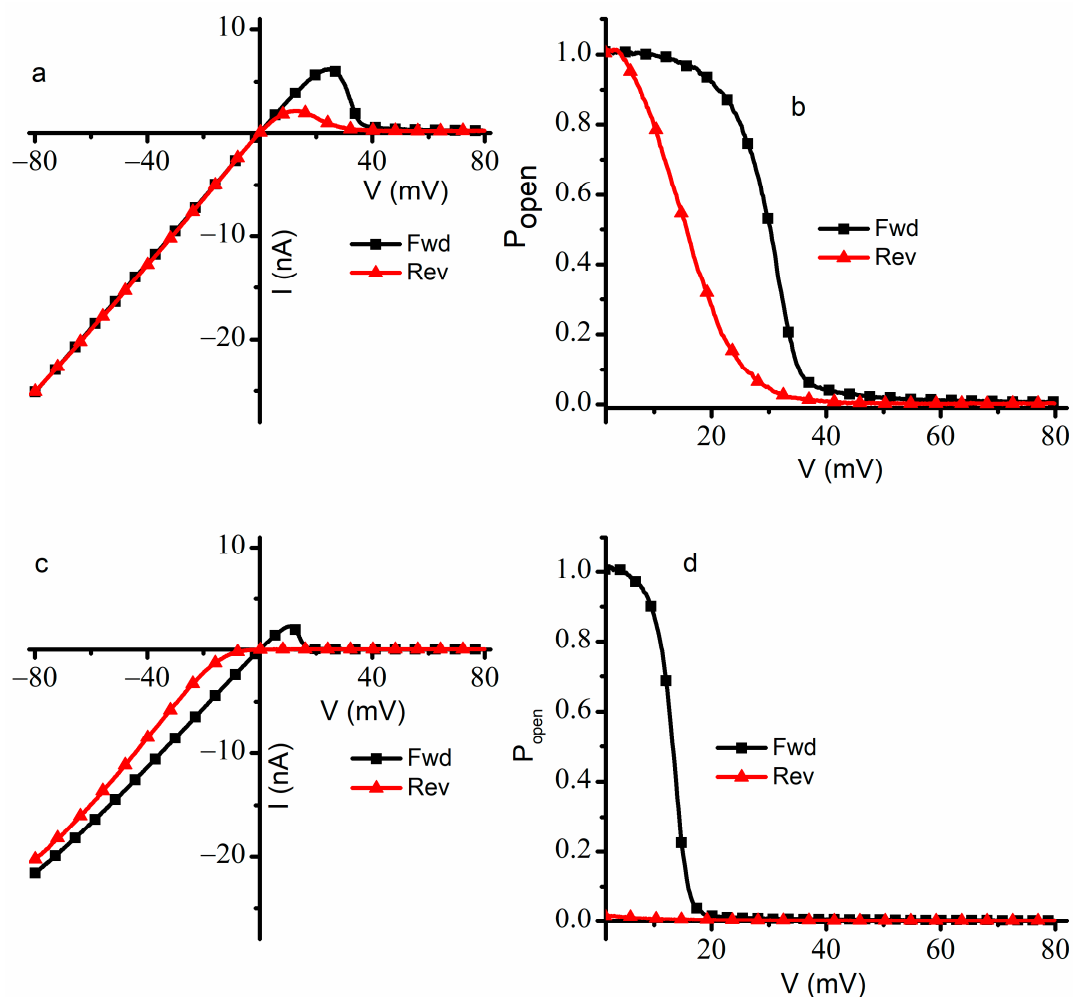


**Figure 3.**  $Cu^{2+}$  ions modulate the voltage gating and hysteresis of lysenin channels for an extended voltage range. In the absence of  $Cu^{2+}$  ions, the hysteresis in conductance in response to ascending and descending voltage ramps is observed for I-V (a) and open probability ( $P_{open}$ ) (b) plots. The changes in the macroscopic currents,  $P_{open}$ , and midway voltage of activation for channels in a previously open state indicate a history-dependent response to applied voltages.  $Cu^{2+}$  addition influences the I-V (c) and  $P_{open}$  (d) plots recorded in response to the oscillatory voltage stimuli. The addition of  $Cu^{2+}$  ions induces a strong leftward shift in gating during ascending voltage ramps and the previously closed channels resist reopening. The traces represent experimental data, from single traces, with the symbols added to facilitate identification.

The observations inferred from the I-V curves recorded in the absence of  $\text{Cu}^{2+}$  ions were confirmed by plots of the open probability ( $P_{\text{open}}$ ) determined in the positive voltage range for ascending and descending ramps (Figure 3b). To calculate the  $P_{\text{open}}$  value, we used the ratio between the measured currents and the theoretical maximal currents estimated for the same population open channels assumed in the open state at each applied voltage [19,33,34]. These theoretical currents were approximated from the slopes of the linear portion of the response to ascending voltages [18,19]. Since a  $P_{\text{open}}$  value of one was obvious at negative voltages and to avoid the division by zero around the origin, the  $P_{\text{open}}$  was plotted only for positive voltages larger than 1.5 mV. During the ascending voltage ramp, the  $P_{\text{open}}$  equaled one at low positive voltages, started decreasing as the voltage increased, and approached zero at transmembrane voltages larger than 50 mV. However, for the descending voltage ramp, the plot was shifted to the left, and a full reopening occurred at voltages of a few mV. The midway voltage of activation  $V_{0.5}$  (i.e., the voltage at which  $P_{\text{open}} = 0.5$ ) [19,35,36] for ascending ramps was estimated at  $\sim 32$  mV, while the descending ramps indicated a smaller  $V_{0.5}$  value of  $\sim 15$  mV, which is consistent with earlier reports on the hysteresis and bistability of lysenin channels subjected to slow oscillatory voltages [18].

Substantial qualitative and quantitative differences were observed when the experiment was repeated in the presence of  $4 \mu\text{M}$   $\text{Cu}^{2+}$  ions added to both sides of the membrane (Figure 3c). As a consequence of the ligand-induced gating presented by the interactions between lysenin channels and  $\text{Cu}^{2+}$  ions [11], the recorded ionic currents were lower for the entire voltage range. The I-V plot recorded during ascending voltage ramps was linear from  $-80$  mV to  $\sim +8$  mV, which is indicative of an ohmic behavior and the absence of voltage-induced gating within this range. We concluded that the  $\text{Cu}^{2+}$  addition adjusted the voltage at which the channels started to close, and gating occurred at much smaller voltages than in the absence of  $\text{Cu}^{2+}$  ions. This is not the typical behavior of lysenin channels exposed to monovalent and multivalent metal cations, for which the addition induces a rightward shift in the voltage gating behavior during ascending voltages [16]. The channels practically closed at  $+20$  mV and remained in this state for applied voltages up to  $+80$  mV.

A peculiar behavior regarding the effects of added  $\text{Cu}^{2+}$  ions was observed during the descending voltage ramps. The ionic currents measured from  $+80$  mV to  $0$  mV were very small, indicating that lysenin channels resisted opening at any positive voltage. This is also contrasted with the typical behavior of lysenin channels exposed to multivalent metal cations, in which case the reactivation pathway, although indicative of hysteresis, is invariant and unaffected by ion additions [16]. The addition of  $\text{Cu}^{2+}$  ions not only elicited an early closing during ascending voltage ramps but also forced the voltage-closed channels to stay in that state for the entire range of positive potentials during descending voltage ramps. In addition, it seems like the channels remained closed even at negative voltages, and sustained reopening began at voltages under  $-10$  mV. The nonlinear shape of the descending I-V plot recorded at negative voltages together with the consistently lower values of the ionic currents suggested that the reopening of the channels continued at negative potentials and that not all the channels reopened within the timeframe of the experiment. Since the channels did not fully reopen during the descending voltage ramp, we used the linear portion of the I-V plot recorded during the ascending voltage ramp as reference to determine  $P_{\text{open}}$  since all the channels, except the ones closed due to ligand gating, were in the open state at negative voltages. The analysis of the  $P_{\text{open}}$  at positive voltages (Figure 3d) confirmed our observations inferred from the I-V plots. The midway voltage of activation  $V_{0.5}$  for the ascending voltage ramp was estimated at  $\sim +15$  mV; however, the  $P_{\text{open}}$  measured for the descending voltage ramp was nearly zero for the entire range of positive voltages.

The experimental investigations of the effects of  $\text{Cu}^{2+}$  ions presented above showed major changes in the hysteresis and bistability of lysenin channels, indicative of memory capabilities. Nonetheless, an important remaining question was the behavior of lysenin channels in the absence of any applied voltage (i.e.,  $0$  mV). The I-V and  $P_{\text{open}}$  plots for ascending ramps suggested a full opening when  $0$  mV was applied to channels that had



previously been in an open state. However, for descending voltage ramps, the plots suggested that at 0 mV, the channels would remain in the closed state if their prior state was closed. To test this assumption, we employed the AC/DC setup presented in the Section 3 and determined the status of the channels regarding various voltages, prior electrical conditions, and conducting states. The resulting recording, taken of a large population of channels without  $\text{Cu}^{2+}$  ions and exposed to simultaneous AC/DC excitation, is shown in Figure 4 for each voltage condition. Before starting the experiment, the channels were biased for a few minutes at  $-60$  mV to ensure that all channels were in the open state. The recording started immediately upon the application of 0 mV DC. In these conditions, the amplitude of the AC current through the  $\sim 2400$  open channels was  $\sim 790$  pA (Figure 3). The manual application of a  $+60$  mV step voltage gradually reduced the amplitude of the AC signal down to  $\sim 375$  pA, indicating a reduction in the macroscopic conductance due to channel closing induced by the applied voltage. After a few minutes, the reapplication of 0 mV led to channel reopening, which was observed as a quick increase in the amplitude of the AC current. In less than one minute, the amplitude of the AC signal recovered the initial value ( $\sim 790$  pA), indicative of a quick reinstatement of the original conductance and full channel reopening. This experiment suggested that, in the absence of  $\text{Cu}^{2+}$  ions, the channels were open at 0 mV, started closing at positive voltages, and rapidly re-instated their initial conductance after removal of the DC voltage stimulus.

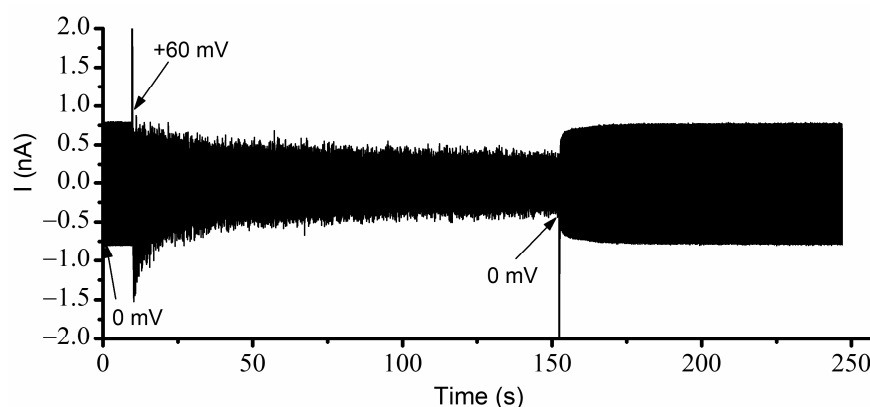


**Figure 4.** Determination of lysenin channels' macroscopic conductance from combined AC/DC stimulation. The application of 0 mV and  $+60$  mV DC voltages is indicated in the figure. The fully open state at 0 mV at the beginning of the recording is indicated by the large value of the AC current amplitude. The decreasing amplitude observed after the application of  $+60$  mV indicates channel closure. The re-application of  $+60$  mV reinstates the fully conducting state, which is indicative of channel reopening.

A few important observations can be made from a further analysis of the channel conductance estimated from the trace shown in Figure 4. Firstly, the signal to noise ratio recorded at 0 mV before and after channel closure seemed much smaller than the one recorded during the application of the  $+60$  mV step voltage. The larger value of the electrical noise while channels were closing most likely originated in the conformational open-close fluctuations manifested during voltage application. At  $+60$  mV, the amplitude of the AC current decreased exponentially (as anticipated) but owing to the large volume of data (sampling frequency 500 Hz), we opted not to wait until a constant amplitude was achieved (i.e., indicative of steady state). Regardless, one may reasonably estimate that many of the channels were still in the open conformation, which was not observed in the I-V and  $P_{\text{open}}$  plots shown in Figures 2 and 3. The explanation for this behavior is related to the high density of the channels in the target membrane [19]. To successfully complete these experiments and obtain a reasonable amplitude of the AC current for a 1 mV stimulation, we needed to reconstitute more channels in the target membrane. However, given the propensity of lysenin to prefer oligomerization into lipid rafts [19,37], high local

channel densities may be achieved with only a few thousand channels, which may lead to adjustments of voltage-induced gating and the prevention of full closing even at high positive voltages [19].

Our next experiment addressed the influence of  $\text{Cu}^{2+}$  ions on lysenin channel's opening, reopening, and bistability in response to applied voltages while accounting for the history of the channels. To do this, we utilized the same experimental system and used the AC currents to determine the status of the channels exposed to  $4 \mu\text{M}$   $\text{Cu}^{2+}$  and additional DC voltages (Figure 5). Before recording, the membrane was biased by  $-60$  mV for several minutes to ensure that all the channels were in the open state. The application of the AC signal at  $0$  mV DC voltage indicated an ionic current amplitude of  $\sim 710$  pA. The application of  $+60$  mV DC to the membrane led to a fast decline of the AC current amplitude to  $\sim 35$  pA. After channel closure, we monitored the amplitude of the AC current at  $0$  mV bias voltage. As the experiment utilized a fast-sampling rate, we recorded a large amount of data. To mitigate potential problems with the acquisition system and further data analysis, we temporarily paused the recording during the experiment while maintaining all other electrical and solution conditions. As Figure 5 shows, a very small number of the lysenin channels previously closed by the application of the  $+60$  mV potential reopened after removing the voltage stimulus. At  $0$  mV, the previously closed channels maintained their state for an extended time, as seen by the notably low AC current amplitude, which was monitored for more than 30 min. The small, stable amplitude of the AC current suggested the channels exposed to  $\text{Cu}^{2+}$  ions and previously closed by voltage remained in the closed state for a remarkably long time, if not indefinitely, at a  $0$  mV bias potential.

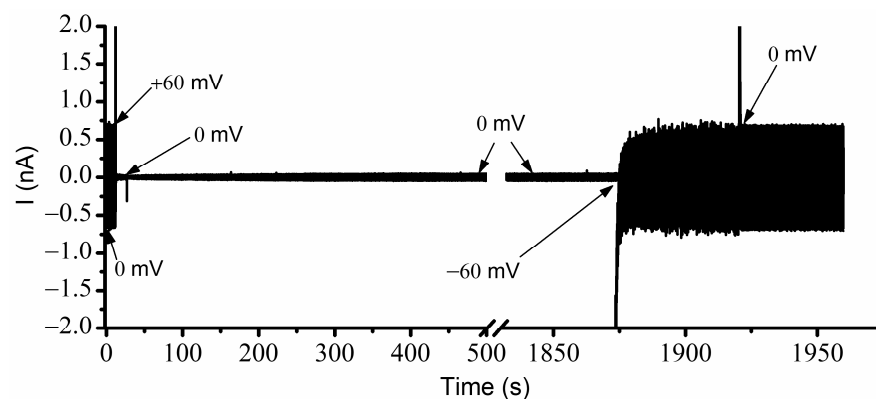


**Figure 5.**  $\text{Cu}^{2+}$  ions adjust the response of lysenin channels to voltages in a history-dependent manner. A large macroscopic conductance at  $0$  mV for previously open channels is indicated by the large amplitude of the AC current. The channels close rapidly at  $+60$  mV but removal of the DC bias voltage does not lead to reopening. The channels reopen upon application of a negative bias voltage step ( $-60$  mV); subsequent removal of the DC stimulus (i.e., reapplication of  $0$  mV) reinstates the current prior to channel closure, demonstrating a bistable system.

To verify if the channels were permanently closed (which would be in contradiction with the results shown in the I-V plots), we applied a  $-60$  mV transmembrane voltage for about one minute, which elicited a fast increase in the AC currents, which was indicative of channel reopening. The same maximum amplitude of the AC current was recorded after a consequent application of  $0$  mV; the recovery of the amplitude of the AC current to the same value we recorded at  $0$  mV before closing the channels suggested that the channels fully reopened upon the application of the hyperpolarization voltage. The power spectrum for each portion of the trace recorded at a particular voltage and channel conformation indicated the presence of the  $10$  Hz AC signal (Figure 6).

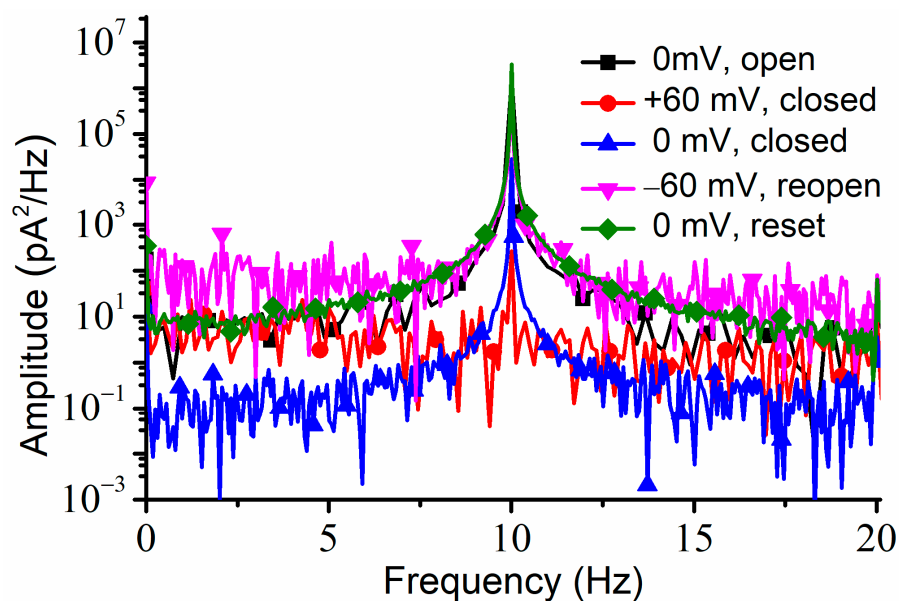


**Figure 6.** The power spectrum recorded for all the voltage and conformation conditions indicate the presence of the 10 Hz AC signal for channels open at 0 mV (squares), closed at +60 mV (circles), closed at 0 mV (up triangles), reopen at −60 mV (down triangles), and again at 0 mV after reopening by the negative step voltage (diamonds). The symbols were added to traces constructed from all the experimental data to facilitate identification.

The experiments indicated that  $\text{Cu}^{2+}$  ions elicit not only major changes in hysteresis but also adjustments of the voltage-elicited response: faster closing, slower reopening, and a left-shifted midway voltage of activation. This is opposite to what is known of the influence of monovalent and trivalent metal cations on lysenin channels, which usually manifests by a rightward shift of the midway voltage of activation and slow down the response to positive voltage stimuli in response to ascending voltage ramps [14,16]. These discrepancies suggest  $\text{Cu}^{2+}$  may present a very different interaction with lysenin channels and act by promoting channel closure even when this feature would be weakened or suppressed by experimental conditions. In this line, lysenin channels are well known for losing their voltage-induced gating upon reconstitution in bilayer lipid membranes composed of electrically neutral lipids [2,11,15]. To investigate the influence of  $\text{Cu}^{2+}$  ions on the voltage gating of lysenin channels reconstituted in neutral bilayers, we employed support lipid membranes in which we replaced the anionic Aso with the neutral Diphytanoil-Phosphatidylcholine (DiPhyt-PC) as the major membrane component [2,11,15]. In these experimental conditions, the suppression of voltage gating for the ~2000 inserted channels was seen in the quasi-linear I-V plot recorded from −60 mV to +60 mV (Figure 7).

The linear I-V plot constructed for lysenin channels reconstituted in neutral membranes and in the absence of  $\text{Cu}^{2+}$  ions indicated that no voltage-induced gating manifested for the entire voltage range employed in this experiment, confirming prior investigations [11,15]. After the addition of  $\text{Cu}^{2+}$  to both sides (4  $\mu\text{M}$  final concentration in each reservoir), the lysenin channels maintained the ohmic behavior for negative voltages and up to ~+10 mV. Surprisingly, the ionic currents decreased significantly for larger positive voltages (exceeding +10 mV), indicative of channel closing by voltage gating. The small values of the ionic currents measured at applied voltages exceeding 20 mV implied that the channels closed completely, suggesting that the  $\text{Cu}^{2+}$  addition restored the voltage gating properties. In addition, the  $P_{\text{open}}$  determined for voltage ramps in the positive voltage range (Figure 7b) indicated a complete recovery of the hysteretic behavior, including the arresting of the channels in the closed state at positive voltages and the absence of reopening at 0 mV.

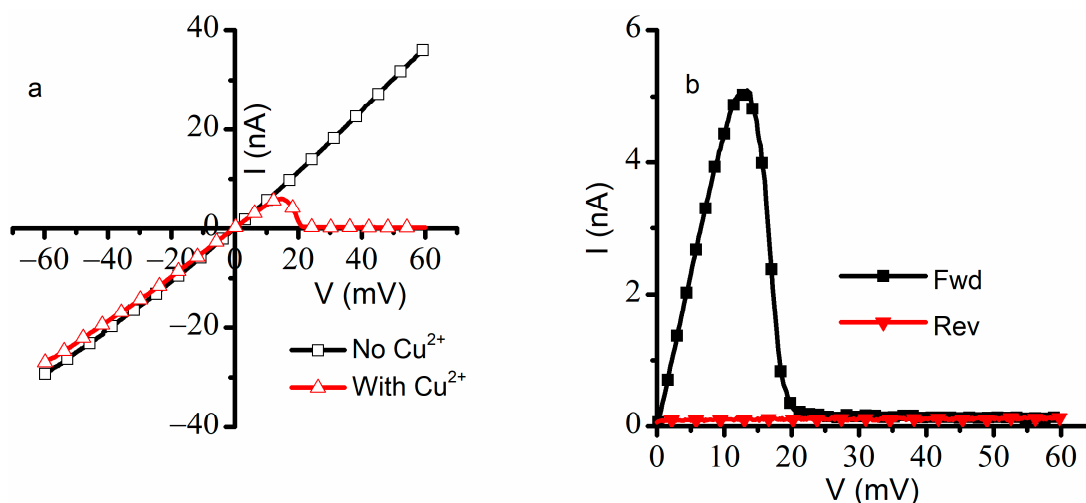


**Figure 7.** Cu<sup>2+</sup> reinstates the voltage gating and hysteresis features of lysenin channels in neutral membranes. The linear I-V plot recorded for lysenin channels reconstituted in neutral membranes ((a), open squares) indicates the absence of voltage-induced gating. The voltage-induced gating feature is reinstated upon Cu<sup>2+</sup> addition ((a), open up triangles). The I-V plot recorded after Cu<sup>2+</sup> addition (b) for ascending (full squares) and descending (full down triangles) voltage ramps indicates the hysteresis in conductance and history-dependent response to applied voltages. The plots represent experimental data from single traces, with the symbols added to facilitate identification.

Our findings raise more questions than provide answers with regard to deciphering the complex gating mechanisms presented by lysenin channels. Voltage gating and its absence in neutral membranes, as well as hysteresis, have been reported for more than two decades [2,18]. Nonetheless, no real progress was encountered regarding the biophysical mechanisms by which they manifest, which makes a mechanistic interpretation of our data difficult. Although electrostatic interactions seem to play a major role in voltage gating (because it is suppressed in neutral membranes, and modulated by ionic strength), how exactly they lead to gating is not known. Our work did not bring any experimental evidence to indicate that the changes in voltage gating and hysteresis are a consequence of the interaction of Cu<sup>2+</sup> ions with lipids, proteins, or both. Cu<sup>2+</sup> ions lead to a leftward shift of the open probability for both ascending and descending voltage ramps, while other monovalent and multivalent metal cations (i.e., K<sup>+</sup> and La<sup>3+</sup>) adjust the hysteresis by a rightward shift of the open probability during ascending voltage ramps and an invariant pathway for descending voltage ramps (channel reopening) [16]. The current structural data [1,3] do not provide sufficient evidence of an outside domain able to occlude the channel by a ball and chain mechanism, but such occurrence may not be fully excluded. While our findings may help in elucidating the mechanism of lysenin's gating, substantial investigations are needed to attain this goal.

On the other hand, we anticipate our findings to contribute to a better understanding of how such behavior may provide molecular memory capabilities to unicellular or even complex organisms. Lysenin is not an ion channel; as a matter of fact, it is not even a transmembrane protein in its native environment. Lysenin shares salient features of ion channels (i.e., high transport rate, regulation, and selectivity), and it is endowed with strong memristive capabilities. The memory originating in the kinetics of ion channels as well as the implications of memristive properties in learning and the establishment of important neural functions are under intense scrutiny for a better understanding of how molecular memory contributes to fundamental physiological processes [20,22,23,32,38–43]. In addition to replicating fundamental features of ion channels, lysenin is much easier to work with, which makes it an excellent experimental model for exploring molecular memory phenomena and their consequences.

### 3. Materials and Methods

The lipids used for these experiments were Asolectin (Aso, Sigma-Aldrich, St. Louis, MO, USA), Sphingomyelin (SM, Avanti Polar Lipids, Alabaster, AL, USA), Diphytanoil-Phosphatidylcholine (Diphyt-PC, Avanti Polar Lipids) and cholesterol (Chol, Sigma-Aldrich). The lipids, which were originally in powder form, were solubilized in *n*-decane (Fisher Scientific, Pittsburgh, PA, USA) to produce lipid mixtures of Aso/SM/Chol at a weight ratio of 10:5:4. Neutral bilayers were prepared by replacing Aso with DiPhyt-PC in the lipid mixture.

The planar lipid membrane experimental setup (Figure 8), often used for electrophysiology investigations on lysenin channels [2,10–12], consisted of two insulating polytetrafluoroethylene (PTFE) reservoirs (each of ~1 mL volume) separated by a thin PTFE film (~120  $\mu\text{m}$  thickness) in which a central hole of ~100  $\mu\text{m}$  diameter was created by an electric spark. The reservoirs were filled with electrolyte solutions made of 50 mM KCl (Fisher Scientific) and 20 mM Hepes (pH 7.2, Sigma-Aldrich). For electrical connections, two Ag/AgCl electrodes embedded in salt bridges (2% low melting point agarose—Sigma Aldrich, dissolved in 1 M NaCl—Fisher Scientific) were inserted directly into the electrolyte solutions in the two reservoirs. The Ag/AgCl electrodes were wired to the headstage of the electrophysiology amplifier (Axopatch 200B, Molecular Devices, San Jose, CA, USA), which fed into the DigiData 1440A digitizer (Molecular Devices). The computer-controlled digitizer was used for online visualization, recording, and further analysis with the pClamp 10.7.0.3 software package (Molecular Devices). The recorded data were further analyzed and plotted with the Origin 8.5.1 (OriginLab, Northampton, MA, USA) software package.

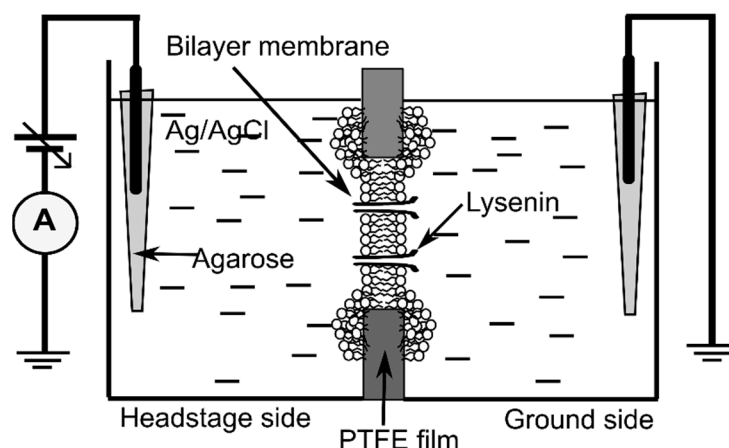


**Figure 8.** The experimental setup for electrophysiology measurements. Lysenin channels are reconstituted in a bilayer lipid membrane (BLM) bathed by electrolyte solutions. The electrical connections to the Axopatch 200B electrophysiology amplifier are ensured by agarose salt bridges and Ag/AgCl electrodes wired to the headstage. The diagram is not to scale.

Membrane formation and stabilization was monitored by estimating the membrane capacitance from the capacitive current measured in response to a triangle-wave signal (provided from a Keithley 3390 function generator), and the seal was verified by applying a DC voltage to the membrane. After a stable membrane was formed ( $C > 65$  pF,  $R > 100$  G $\Omega$ ), we proceeded with channel insertion. Small amounts of recombinant lysenin [12] were added to the grounded reservoir under continuous stirring (Warner Instruments low noise magnetic stirrer) and upon application of  $-60$  mV bias potential (manual command). Channel insertion was recorded at 10 Hz sampling frequency and monitored from the stepwise variation of the ionic currents measured at constant voltage [2,10,13,14]. After achieving a steady state of the macroscopic current in ~2 h, we proceeded with electrophysiology measurements before and after  $\text{Cu}^{2+}$  additions. For this purpose, we used a 1 M  $\text{CuSO}_4$  stock solution (Fisher Scientific) after proper serial dilution in buffered electrolyte solutions. After  $\text{Cu}^{2+}$  addition to both sides of the membrane (4  $\mu\text{M}$  final concentration for all experi-

ments), we maintained stirring for several minutes to allow mixing and enable interactions between channels and ions.

Linear voltage ramps were created with the digitizer by defining proper episodic stimulation protocols [14,18]. For data recording, we used a 1 kHz low-pass hardware filter, 100 Hz low-pass software filter, and a sampling frequency of 1 Hz.

To determine the status of the channels (i.e., open/closed) at any voltage (including zero voltage), we created an experimental setup that applied simultaneous AC and DC to the membrane. The DC voltage, utilized to control the status of the channels, was applied to the bilayer membrane with the manual command of the instrument, while the AC signals (10 Hz, 1 mV amplitude sine wave), utilized to estimate the status of the channels, were applied from the function generator via the external input of the electrophysiology amplifier (Figure 9). The unfiltered current included both AC and DC components, with each one dependent on the conductance of the channel population. The application of a high-pass 2 Hz filter suppressed the DC current component; the amplitude of the resulting AC current component was used to estimate the conductance status of the channels at any applied DC voltage.

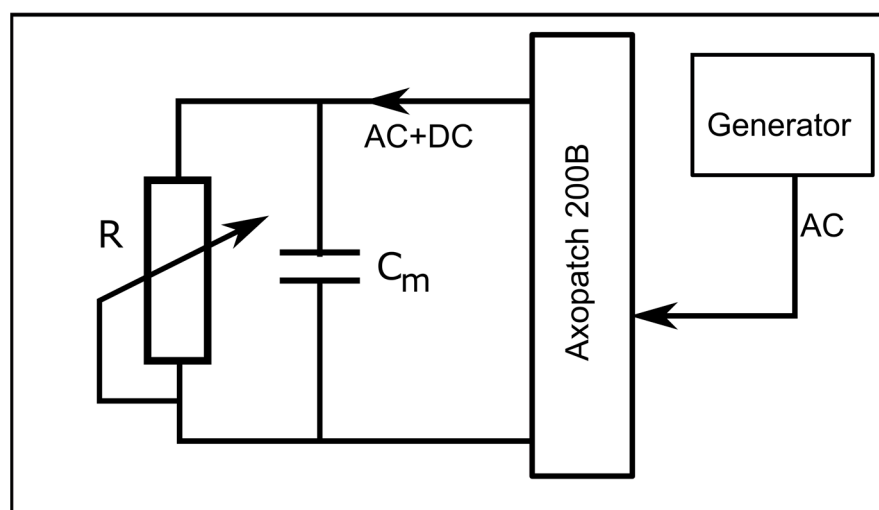


**Figure 9.** Experimental setup for investigating the status of the channels at any applied DC voltage. A combined AC/DC signal is applied from the electrophysiology amplifier to the membrane depicted as a capacitor  $C_m$  in parallel to a variable resistor  $R$  (the conducting pathway created by inserted lysenin channels).

The amplitude of the AC signal was chosen to be very small (i.e., 1 mV) to prevent channel closing by voltage (which may not occur at very low positive voltages, or fast sweeps [18]), yet it was large enough to detect AC currents through open channels. Also, the low amplitude and frequency prevented attaining large values of the capacitive currents; for a 100 pF membrane, the amplitude of the capacitive current estimated for these experimental conditions would be less than 10 pA. To avoid excessive chopping or filtering of the AC signal, we utilized a sampling time of 2 msec, a 10 kHz low-pass hardware filter, and no other low-pass software filter.

#### 4. Conclusions

Our work showed that the addition of very small amounts of  $\text{Cu}^{2+}$  ions to the bulk electrolyte solutions had multiple effects on the voltage gating profile of lysenin channels. Earlier reports showed that lysenin channels reconstituted into lipid membranes containing anionic lipids present a strong hysteresis in conductance manifested as a preference for the previously attained closed state. This hysteresis did not originate in the slow equilibration of the channels since it persisted for periods of the oscillatory stimulus that greatly exceeded the relaxation time of the channels. In this work, we utilized traditional I-V measurements

together with an improved experimental setup and showed that  $\text{Cu}^{2+}$  addition modifies the gating profile and substantially affects the response to oscillatory stimuli. Unlike other multivalent ions,  $\text{Cu}^{2+}$  potentiated the voltage-induced gating and open-close channel transitions were attained at smaller potentials. These effects were more pronounced for the close–open transitions: during descending voltage ramps, the channels did not reopen even at 0 mV bias potential (such measurements were made possible by using a new experimental setup), and large hyperpolarizing voltages were needed to reinstate the open channel conductance. The history-dependent transitions between conformations led to bistability, caused a strong hysteresis in conductance, and endowed the channels with potential memory capabilities. An interesting fact is that this molecular memory can be fully addressed by employing electrical signals for writing, reading, and erasing it. Lysenin channels behave like true biological memristors but the molecular mechanisms by which such intricate functions are attained are yet to be deciphered.

**Author Contributions:** Conceptualization, A.B. and D.F.; methodology, A.B., A.R.S. and D.F.; software, P.W.F., I.M.F., A.B., A.R.S. and D.F.; validation, A.B., R.W. and D.F.; investigation, A.B., P.W.F., I.M.F., A.R.S., R.W. and D.F.; lysenin production and purification, R.W.; resources, D.F.; supervision and project administration, A.B. and D.F. All authors contributed to original draft preparation, review, editing. All authors have read and agreed to the published version of the manuscript.

**Funding:** This research was funded by the National Science Foundation (grant number 1554166) and National Institute of Health (grant numbers P20GM103408 and P20GM109095).

**Institutional Review Board Statement:** Not applicable.

**Informed Consent Statement:** Not applicable.

**Data Availability Statement:** The data presented in this study are available on request from the corresponding author.

**Acknowledgments:** I.M.F., a student at Leland High School, San Jose, CA, USA, contributed to experimental and theoretical approaches of this work during a summer 2022 internship at Boise State University.

**Conflicts of Interest:** The authors declare no conflict of interest. The funders had no role in the design of the study; in the collection, analyses, or interpretation of data; in the writing of the manuscript, or in the decision to publish the results.

## References

1. Bokori-Brown, M.; Martin, T.G.; Naylor, C.E.; Basak, A.K.; Titball, R.W.; Savva, C.G. Cryo-EM structure of lysenin pore elucidates membrane insertion by an aerolysin family protein. *Nat. Commun.* **2016**, *7*, 11293. [[CrossRef](#)] [[PubMed](#)]
2. Ide, T.; Aoki, T.; Takeuchi, Y.; Yanagida, T. Lysenin forms a voltage-dependent channel in artificial lipid bilayer membranes. *Biochem. Biophys. Res. Commun.* **2006**, *346*, 288–292. [[CrossRef](#)] [[PubMed](#)]
3. Podobnik, M.; Savory, P.; Rojko, N.; Kisovec, M.; Wood, N.; Hambley, R.; Pugh, J.; Wallace, E.J.; McNeill, L.; Bruce, M.; et al. Crystal structure of an invertebrate cytolysin pore reveals unique properties and mechanism of assembly. *Nat. Commun.* **2016**, *7*, 11598. [[CrossRef](#)] [[PubMed](#)]
4. Shakor, A.-B.A.; Czurylo, E.A.; Sobota, A. Lysenin, a unique sphingomyelin-binding protein. *FEBS Lett.* **2003**, *542*, 1–6. [[CrossRef](#)] [[PubMed](#)]
5. Shogomori, H.; Kobayashi, T. Lysenin: A sphingomyelin specific pore-forming toxin. *Biochim. Biophys. Acta* **2008**, *1780*, 612–618. [[CrossRef](#)] [[PubMed](#)]
6. Yamaji-Hasegawa, A.; Makino, A.; Baba, T.; Senoh, Y.; Kimura-Suda, H.; Sato, S.B.; Terada, N.; Ohno, S.; Kiyokawa, E.; Umeda, M.; et al. Oligomerization and pore formation of a sphingomyelin-specific toxin, lysenin. *J. Biol. Chem.* **2003**, *278*, 22762–22770. [[CrossRef](#)]
7. Yilmaz, N.; Kobayashi, T. Visualization of Lipid membrane Reorganization Induced by a Pore-Forming Toxin Using High-Speed Atomic Force Microscopy. *ACS Nano* **2015**, *9*, 7960–7967. [[CrossRef](#)]
8. Yilmaz, N.; Yamada, T.; Greimel, P.; Uchihashi, T.; Ando, T.; Kobayashi, T. Real-Time Visualization of Assembling of a Sphingomyelin-Specific Toxin on Planar Lipid Membranes. *Biophys. J.* **2013**, *105*, 1397–1405. [[CrossRef](#)]
9. Yilmaz, N.; Yamaji-Hasegawa, A.; Hullin-Matsuda, F.; Kobayashi, T. Molecular mechanisms of action of sphingomyelin-specific pore-forming toxin, lysenin. *Semin. Cell Dev. Biol.* **2018**, *73*, 188–198. [[CrossRef](#)]

10. Kwiatkowska, K.; Hordejuk, R.; Szymczyk, P.; Kulma, M.; Abdel-Shakor, A.-B.; Plucienniczak, A.; Dolowy, K.; Szewczyk, A.; Sobota, A. Lysenin-His, a sphingomyelin-recognizing toxin, requires tryptophan 20 for cation-selective channel assembly but not for membrane binding. *Mol. Membr. Biol.* **2007**, *24*, 121–134. [[CrossRef](#)]
11. Bogard, A.; Abatchev, G.; Hutchinson, Z.; Ward, J.; Finn, P.W.; McKinney, F.; Fologea, D. Lysenin Channels as Sensors for Ions and Molecules. *Sensors* **2020**, *20*, 6099. [[CrossRef](#)] [[PubMed](#)]
12. Bogard, A.; Finn, P.W.; McKinney, F.; Flacau, I.M.; Smith, A.R.; Whiting, R.; Fologea, D. The Ionic Selectivity of Lysenin Channels in Open and Sub-Conducting States. *Membranes* **2021**, *11*, 897. [[CrossRef](#)] [[PubMed](#)]
13. Fologea, D.; Krueger, E.; Al Faori, R.; Lee, R.; Mazur, Y.I.; Henry, R.; Arnold, M.; Salamo, G.J. Multivalent ions control the transport through lysenin channels. *Biophys. Chem.* **2010**, *152*, 40–45. [[CrossRef](#)]
14. Fologea, D.; Krueger, E.; Lee, R.; Naglak, M.; Mazur, Y.; Henry, R.; Salamo, G. Controlled gating of lysenin pores. *Biophys. Chem.* **2010**, *146*, 25–29. [[CrossRef](#)] [[PubMed](#)]
15. Fologea, D.; Al Faori, R.; Krueger, E.; Mazur, Y.I.; Kern, M.; Williams, M.; Mortazavi, A.; Henry, R.; Salamo, G.J. Potential analytical applications of lysenin channels for detection of multivalent ions. *Anal. Bioanal. Chem.* **2011**, *401*, 1871–1879. [[CrossRef](#)]
16. Bryant, S.L.; Clark, T.; Thomas, C.A.; Ware, K.S.; Bogard, A.; Calzacorta, C.; Prather, D.; Fologea, D. Insights into the Voltage Regulation Mechanism of the Pore-Forming Toxin Lysenin. *Toxins* **2018**, *10*, 334. [[CrossRef](#)]
17. Krueger, E.; Al Faouri, R.; Fologea, D.; Henry, R.; Straub, D.; Salamo, G. A model for the hysteresis observed in gating of lysenin channels. *Biophys. Chem.* **2013**, *184*, 126–130. [[CrossRef](#)]
18. Fologea, D.; Krueger, E.; Mazur, Y.I.; Stith, C.; Okuyama, Y.; Henry, R.; Salamo, G.J. Bi-stability, hysteresis, and memory of voltage-gated lysenin channels. *Biochim. Biophys. Acta Biomembr.* **2011**, *1808*, 2933–2939. [[CrossRef](#)]
19. Krueger, E.; Bryant, S.; Shrestha, N.; Clark, T.; Hanna, C.; Pink, D.; Fologea, D. Intramembrane congestion effects on lysenin channel voltage-induced gating. *Eur. Biophys. J.* **2016**, *45*, 187–194. [[CrossRef](#)]
20. Villalba-Galea, C.A. Hysteresis in voltage-gated channels. *Channels* **2017**, *11*, 140–155. [[CrossRef](#)]
21. Pustovoit, M.A.; Berezhkovskii, A.M.; Bezrukov, S.M. Analytical theory of hysteresis in ion channels: Two state model. *J. Chem. Phys.* **2006**, *125*, 194907. [[CrossRef](#)]
22. Pfeiffer, P.; Egorov, A.V.; Lorenz, F.; Schleimer, J.-H.; Draguhn, A.; Schreiber, S. Clusters of cooperative ion channels enable a membrane-potential-based mechanism for short-term memory. *eLife* **2020**, *9*, e49974. [[CrossRef](#)] [[PubMed](#)]
23. Villalba-Galea, C.A.; Chiem, A.T. Hysteretic Behavior in Voltage-Gated Channels. *Front. Pharmacol.* **2020**, *11*, 579596. [[CrossRef](#)] [[PubMed](#)]
24. Chua, L.O.; Kang, S.M. Memristive Devices and Systems. *Proc. IEEE* **1976**, *64*, 209–223. [[CrossRef](#)]
25. Strukov, D.B.; Snider, G.S.; Stewart, D.R.; Williams, R.S. The missing memristor found. *Nature* **2008**, *453*, 80–83. [[CrossRef](#)]
26. Andersson, T. Exploring voltage-dependent ion channels in silico by hysteretic conductance. *Math. Biosci.* **2010**, *226*, 16–27. [[CrossRef](#)]
27. Bennekou, P.; Barksman, T.L.; Jensen, L.R.; Kristensen, B.I.; Christophersen, P. Voltage activation and hysteresis of the non-selective voltage-dependent channel in the intact human red cell. *Bioelectrochemistry* **2004**, *62*, 181–185. [[CrossRef](#)]
28. Kaestner, L.; Christophersen, P.; Bernhardt, I.; Bennekou, P. The non-selective voltage-activated cation channel in the human red blood cell membrane: Reconciliation between two conflicting reports and further characterization. *Bioelectrochemistry* **2000**, *52*, 117–125. [[CrossRef](#)]
29. Mannikko, R.; Pandey, S.; Larsson, H.P.; Elinder, F. Hysteresis in the Voltage Dependence of HCN Channels: Conversion between Two Modes Affects Pacemaker Properties. *J. Gen. Physiol.* **2005**, *125*, 305–326. [[CrossRef](#)]
30. Nowak-Gudowska, E.; Flyvbjerg, H.; Bennekou, P.; Christophersen, P. Hysteresis in Channel Gating. In *Unsolved Problems of Noise and Fluctuations: UPoN 2002: Third International Conference, CP665*; Bezrukov, S.M., Ed.; AIP: Washington, DC, USA, 2002; pp. 305–311.
31. Bryant, S.; Shrestha, N.; Carnig, P.; Kosydar, S.; Belzeski, P.; Hanna, C.; Fologea, D. Purinergic control of lysenin's transport and voltage-gating properties. *Purinergic Signal.* **2016**, *12*, 549–559. [[CrossRef](#)]
32. Rappaport, S.M.; Teijido, O.; Hoogerheide, D.P.; Rostovtseva, T.K.; Berezhkovskii, A.M.; Bezrukov, S.M. Conductance hysteresis in the voltage-dependent anion channel. *Eur. Biophys. J.* **2015**, *44*, 465–472. [[CrossRef](#)] [[PubMed](#)]
33. Bezanilla, F. Voltage-gated ion channels. *IEEE Trans. NanoBiosci.* **2005**, *4*, 34–48. [[CrossRef](#)] [[PubMed](#)]
34. Tao, X.; Lee, A.; Limapichat, W.; Dougherty, D.A.; MacKinnon, R. A Gating Charge Transfer Center in Voltage Sensors. *Science* **2010**, *328*, 67–73. [[CrossRef](#)] [[PubMed](#)]
35. Latorre, R.; Vargas, G.; Orta, G.; Brauchi, S. Voltage and Temperature Gating of ThermoTRP Channels. In *TRP Ion Channel Function in Sensory Transduction and Cellular Signaling Cascades*; Liedte, W.B., Heller, S., Eds.; CRC Press: Boca Raton, FL, USA, 2007.
36. Phillips, R.; Ursell, T.; Wiggins, P.; Sens, P. Emerging roles for lipids in shaping membrane-protein function. *Nature* **2009**, *459*, 379–385. [[CrossRef](#)]
37. Kulma, M.; Hereć, M.; Grudziński, W.; Anderluh, G.; Gruszecki, W.I.; Kwiatkowska, K.; Sobota, A. Sphingomyelin-rich domains are sites of lysenin oligomerization: Implications for raft studies. *Biochim. Biophys. Acta* **2010**, *1798*, 471–481. [[CrossRef](#)]
38. Koner, S.; Najem, J.S.; Hasan, M.S.; Sarles, S.A. Memristive plasticity in artificial electrical synapses via geometrically reconfigurable, gramicidin-doped biomembranes. *Nanoscale* **2019**, *11*, 18640–18652. [[CrossRef](#)]
39. Najem, J.S.; Taylor, G.J.; Weiss, R.J.; Hasan, M.S.; Rose, G.; Schuman, C.D.; Belianinov, A.; Collier, C.P.; Sarles, S.A. Memristive Ion Channel-Doped Biomembranes as Synaptic Mimics. *ACS Nano* **2018**, *12*, 4702–4711. [[CrossRef](#)]
40. Pershin, Y.V.; La Fontaine, S.; Di Ventra, M. Memristive model of amoeba learning. *Phys. Rev. E* **2009**, *80*, 21926. [[CrossRef](#)]



41. Silva, M.P.; Rodrigues, C.G.; Varanda, W.A.; Nogueira, R.A. Memory in Ion Channel Kinetics. *Acta Biotheor.* **2021**, *69*, 697–722. [[CrossRef](#)]
42. Cowgill, J.; Chanda, B. Charge-voltage curves of Shaker potassium channel are not hysteretic at steady state. *J. Gen. Physiol.* **2023**, *155*, e202112883. [[CrossRef](#)]
43. Shi, Y.P.; Thouta, S.; Claydon, T.W. Modulation of hERG K<sup>+</sup> Channel Deactivation by Voltage Sensor Relaxation. *Front. Pharmacol.* **2020**, *11*, 139. [[CrossRef](#)] [[PubMed](#)]

**Disclaimer/Publisher's Note:** The statements, opinions and data contained in all publications are solely those of the individual author(s) and contributor(s) and not of MDPI and/or the editor(s). MDPI and/or the editor(s) disclaim responsibility for any injury to people or property resulting from any ideas, methods, instructions or products referred to in the content.